Chemical Physics 39 (1979) 209–220
© North-Holland Publishing Company

SPECTROSCOPIC AND OPTICALLY DETECTED MAGNETIC RESONANCE STUDIES OF PO_2^- IN POTASSIUM CHLORIDE. I. ELECTRONIC AND VIBRATIONAL STATES

S.J. HUNTER, K.W. HIPPS and A.H. FRANCIS
Department of Chemistry, University of Michigan, Ann Arbor, Michigan 48109, USA

Received 29 November 1978

The phosphorescence and phosphorescence excitation spectra of phosphorus activated single crystals of potassium chloride have been examined at 4.2 K. The "color center" responsible for the blue emission in these samples is identified as PO_2^- by isotopic substitution and optically detected magnetic resonance measurements. The observed vibrational frequencies of the PO_2^- ion have been used to compute the normal coordinates of the ground state totally symmetric modes as well as the valuence angle in the valence force approximation. The vibrational analysis of the phosphorescence spectrum has been used together with the computed ground state normal coordinate description to compute the geometrical changes associated with excitation to the lowest triplet state of PO_2^-. The results for PO_2^- are compared with the results of similar calculations and measurements for other 18-electron AB_2 type molecules of the isoelectronic sequence PO_2^-, SO_2, NO_2^- and O_3.

1. Introduction

The optical and vibrational spectra of small molecular ions trapped substitutionally in alkali halide lattices have been an area of active research for the last fifty years. The reasons for this intense interest are undoubtedly numerous and varied but include principally the following: (1) alkali halide crystals are produced easily with high purity and good mechanical and optical qualities; (2) several molecular ions, normally unstable or extremely reactive, may be isolated for spectroscopic investigation in alkali halide lattices where they are evidently stabilized by the crystal field; (3) considerable information may be obtained about the impurity ion and the details of its interaction with the lattice from the analysis of these spectra.

Considering the extensive literature on the subject of the spectroscopy of molecular ions in alkali halide lattices, it is perhaps surprising that a recent review [1] lists only a dozen molecular ion centers for which spectra have been obtained and analyzed in detail. Of the molecular ions which have been studied, most are simple diatomics of which O_2^- is perhaps the most extensively investigated example [2–34]. Far fewer triatomic ions have been investigated and of these the literature is most extensive for NO_2^- [35–62]. There are only several examples of tetratomic centers [46,63] and, without exception, the experimental data available is preliminary and lacking in detail.

The spectra of molecular ions in alkali halide lattices exhibit several features essentially unique to this type of sample. Of these features, two are of particular interest in the present study: the unusually large magnitude of electron–phonon coupling [10] and the property of photo-reorientation [3,5,17]. Both of these topics are discussed in detail in a subsequent article (part III).

This investigation was originally undertaken in an attempt to apply the methods of optically detected magnetic resonance (ODMR) [64–71] to the study of "color centers" in ionic lattices. It is immediately apparent from even a cursory examination of the literature on "color centers" that as late as 1950 optical methods of spectroscopy alone had produced relatively little advance upon Pohl's original investigations [72–75]. The application of ESR spec-

troscopy to the identification and characterization of "color centers" during the decade of the sixties produced far greater advances in the field than had been achieved in the preceding half century. Subsequently, ESR spectroscopy has proved of extraordinary value in the study of molecular ion "centers" in alkali halide lattices, as exemplified best by Kanzig's investigation of the O_2^- center [3,9,15].

In view of the success of ESR as a technique for the study of the ground state dynamics of "color centers" and molecular ions in alkali halide lattices, it does not seem unreasonable to hope that optically detected magnetic resonance could be equally successful in the study of the electronically excited (paramagnetic) states of such centers. In 1973 Marrone et al. [22] and Wasiela et al. [23] successfully used high field optically detected magnetic resonance in the study of self-trapped exciton states in KBr by monitoring recombinant emission from the triplet state of Br_2^- centers.

The recent reports [58–62] of a new molecular ion center formed in alkali halide lattices by heating in phosphorus vapors suggested an interesting further application for the ODMR technique. This study was brought to a successful conclusion in that the chemical identity of the center was established, the approximate geometrical details of the ion obtained, the orientation of the molecular axes in the alkali halide lattice determined, and the magnetic resonance fine structure and hyperfine structure parameters measured. Additionally, certain dynamical properties of the center were observed which have been fully characterized. The total of this work is reported in three parts, of which this is the first and deals solely with the details of the spectroscopic analysis. Part II is concerned with the ODMR investigation and part III with the analysis of photo-reorientation of PO_2^- centers. Some aspects of the ODMR study which support the spectroscopic analysis are introduced in the present paper, with detailed discussion deferred to part II.

The spectroscopic investigation consists of a vibronic analysis of PO_2^- phosphorescence in KCl at 4.2 K, assignment of the three normal modes of vibration in the ground electronic state, determination of the polarization of the absorption and emission spectra of the center, assignment of the orbital symmetry of the first triplet and first singlet excited states, and an approximate assessment of the geometry of the first excited triplet state.

2. Experimental

Single crystal samples of phosphorus activated potassium chloride, yielding essentially identical spectroscopic results, were prepared by two different techniques. In the first procedure, that due to Plachenov [61,62], high purity alkali halide together with about 0.1% by weight of red phosphorus was sealed under vacuum in a vitreous silica tube. The sample tube was then lowered at a rate of approximately 1 cm/h through a high temperature Bridgman furnace. In this manner large single crystals of phosphorus activated alkali halide were obtained. Considerable etching of the fused silica tube by the phosphorus at elevated temperatures was apparent.

In the second method, single crystals of high purity potassium chloride, prepared in fused silica tubes under vacuum by the Bridgman method, were sealed in a fused silica tube together with a small amount of red phosphorus [46]. The tube was then heated for a period of 36–48 hours at 725 C. Upon cooling to room temperature, the crystals were found to be phosphorus activated with the activation confined to a depth of about 1 mm below the exposed crystal surface.

Oxygen-18 enriched crystals were prepared by a two step modification of the above procedures. High purity potassium chloride was fully out-gassed under high vacuum. The outgassed salt was held in the molten phase for 1 h under a 40 mm pressure of 95 atom % $H_2{}^{18}O$ and then allowed to crystallize over a period of about 30 min. The crystalline material prepared in this manner was found to exhibit the yellow emission characteristic of O_2^- ion. Vibrational analysis of the emission spectrum obtained at 5 K showed only $(^{18}O)_2^-$ ion to be present. Material prepared in this fashion was then activated with phosphorus by the vapor activation process described above.

Crystals selected for study were cleaved parallel to the principal cleavage directions of the cubic lattice, mounted in a slow wave microwave helix attached to the end of a length of semi-rigid cryogenic coaxial cable and cooled to the working temperature by either a 1 atm helium exchange gas or direct immersion in superfluid liquid helium. Phosphorescence was excited by the output of a 1 Kw Xenon arc lamp monochromated by a one-half meter McPherson-GCA scanning monochromator with a first order resolving power of about 60 000 .The phosphorescence-excitation spectra were

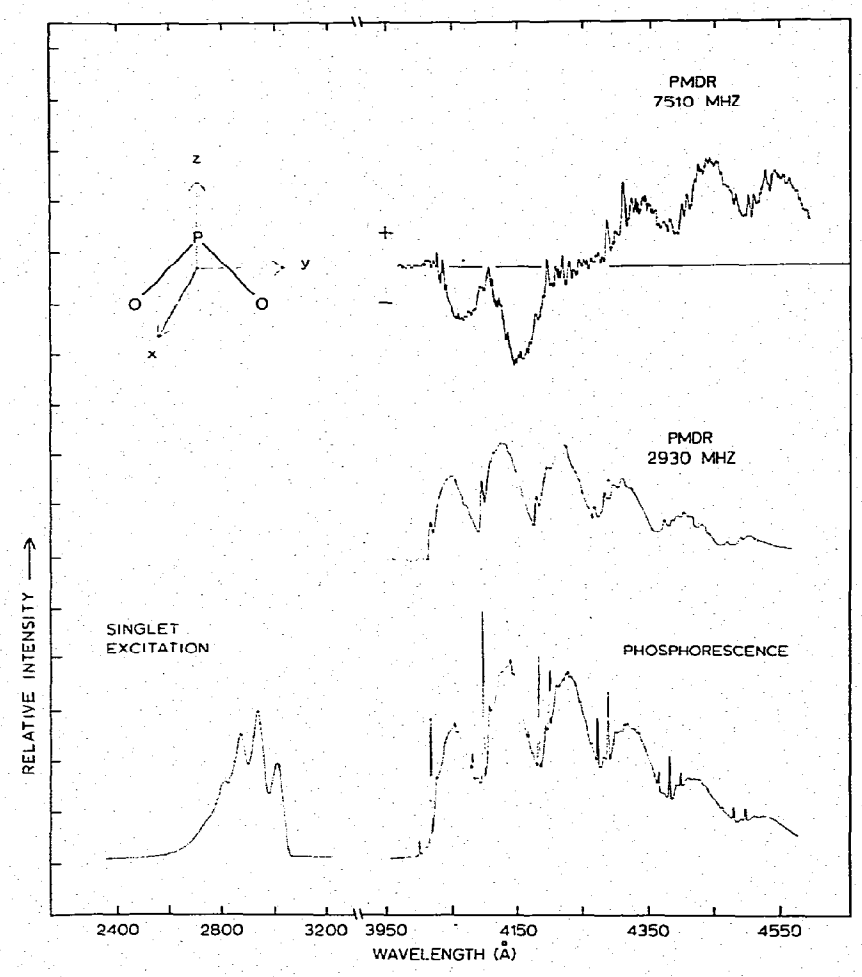

Fig. 1. 7510 MHz and 2930 MHz phosphorescence microwave double resonance (PMDR) spectra, phosphorescence spectrum and phosphorescence excitation spectrum of phosphorus activated potassium chloride single crystal at 4.2 K.

recorded using this instrument with an 8 Å bandpass. Phosphorescence spectra were recorded in the first order of an *f*/8.7 Jarrell–Ash Czerny–Turner scanning monochromator with about 120 000 resolving power using a 1 Å bandpass.

The source of frequency swept microwave radiation employed for the phosphorescence microwave double resonance spectra was a Hewlett–Packard 8690B sweeper and associated plug-in modules. Lifetime measurements were made using the doubled 5900 Å output from a pulsed chromatix CMX-4 dye laser. Decay curves for the lifetime measurements were averaged with a Northern NS575 CAT.

3. Results

The phosphorescence spectrum obtained from phosphorus activated potassium chloride crystals has been published previously by Avarmaa [59] and by ourselves [60] and is reproduced in figs. 1 and 2 together with two PMDR spectra obtained by amplitude modulation of microwave power resonant with the triplet zero-field resonances observed at 2930 MHz and 7510 MHz. An additional weak feature observed 102 cm^{-1} to higher energy of the emission origin is due to phosphorescence from an additional site of unknown structure. Emission from this site is enhanced

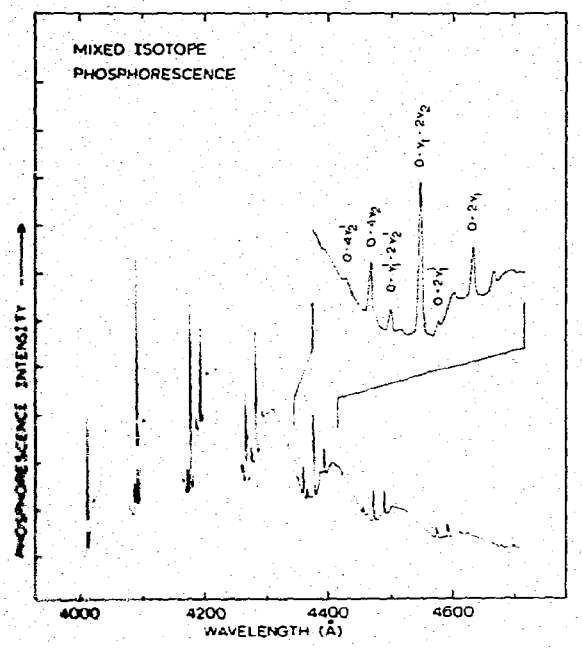

Fig. 2. Phosphorescence spectrum of a phosphorus activated potassium chloride single crystal containing only $(^{18}O)_2^-$ centers.

by doping with a large excess of phosphorus and is absent at low phosphorus levels. The vibronic analysis of the emission from this site is substantially the same as that for emission from the dominant site.

The results of time resolved experiments are shown in figs. 3 and 4. Curve (a) of fig. 3 is a logarithmic plot of the decay of the phosphorescence intensity subsequent to pulsed laser excitation at 4.2 K. The graphical decomposition of the decay curve illustrated in the figure yields spin-orbital state lifetimes in good agreement with those obtained by microwave induced delayed phosphorescence (MIDP). Curves (b) and (c) of fig. 3 are logarithmic plots of the MIDP intensity versus time obtained pumping the 2930 MHz zero-field transition subsequent to pulsed laser excitation and decay of the short lived component of curve (a). The experimental methods used to obtain this data have been discussed in detail previously by several authors [64,65]. Curve (b) is a logarithmic plot of the envelope of the MIDP peaks obtained at different delays. Curve (c) is a logarithmic plot of the decay of an individual delayed MIDP peak. Curves (b) and (c) are the limiting slopes of the composite decay curve shown in curve (a) and yield the lifetimes of the individual spin-orbital states. The experimental MIDP data

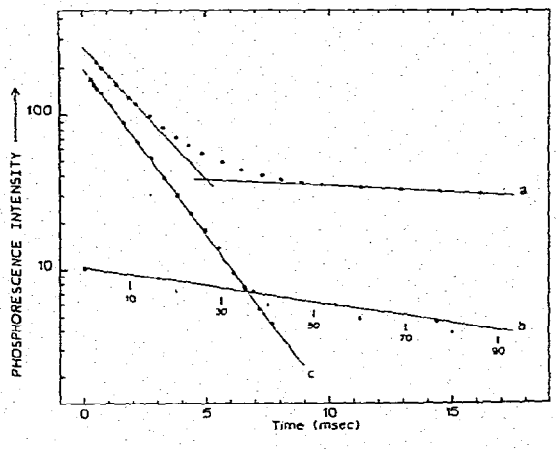

Fig. 3. Curve (a): logarithmic plot of the phosphorescence intensity decay of phosphorus activated KCl at 4.2 K. Curve (c): logarithmic plot of the decay of microwave induced delayed phosphorescence (MIDP) intensity. Curve (b): logarithmic plot of the MIDP envelope.

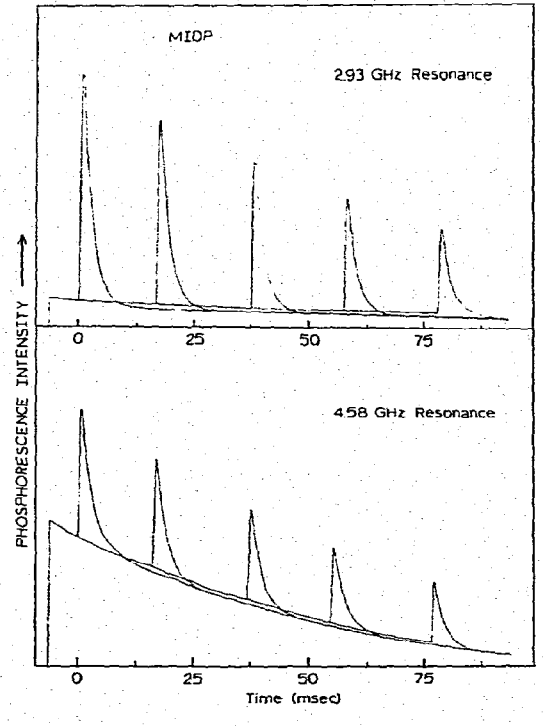

Fig. 4. 4580 MHz and 2930 MHz MIDP envelopes.

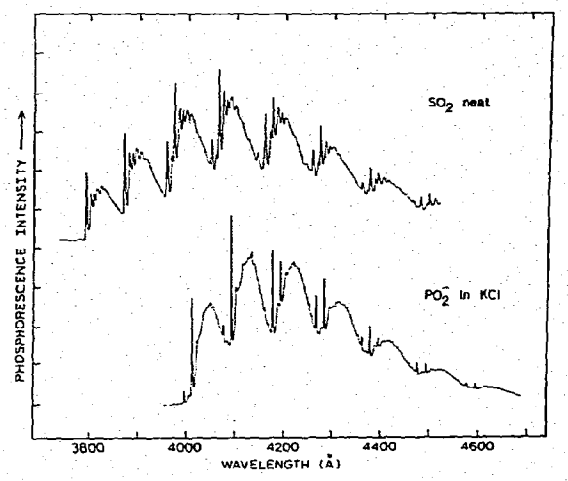

Fig. 5. Comparison of the low temperature phosphorescence spectra of SO_2 (polycrystalline) and PO_2^- (in KCl).

is shown in fig. 4 for both the 4580 MHz and the 2930 MHz transitions.

4. Discussion

4.1. Electronic transitions

The emission spectrum of phosphorus activated potassium chloride crystals at liquid helium temperatures consists of two progressions with vibrational intervals of 501 cm^{-1} and 1097 cm^{-1}. The general appearance of the vibrational envelope is that of a Franck–Condon forbidden transition and bears a marked similarity to the emission spectrum of SO_2. (see fig. 5). Largely on the strength of this similarity, it has been suggested that the impurity center responsible for emission in phosphorus activated alkali halides is the molecular ion PO_2^-, which, although it is isoelectronic with both SO_2 and NO_2^-, is a previously unobserved species.

The long wavelength valence electron transition of an 18-electron AB_2 triatomic molecule may be discussed with the aid of the schematic molecular orbital energy level diagram shown in fig. 6, which has been constructed in the following manner. A set of four group orbitals constructed from the in-phase and out-of-phase oxygen p_σ and p_π atomic orbitals is illustrated on the right of the diagram. On the left side

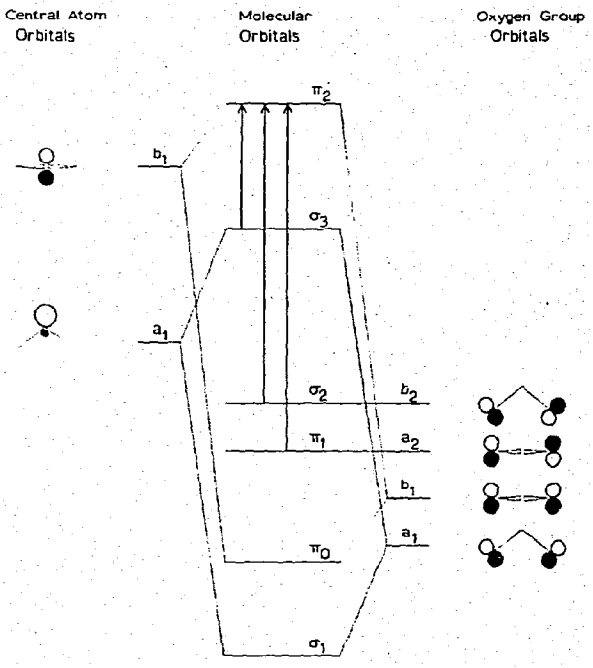

Fig. 6. Schematic representation of the one-electron σ and π molecular orbitals of an AB_2 molecule or ion with 18 valence electrons.

of the diagram are the two central atom atomic orbitals: a p_π and an sp_σ^2 hybrid orbital. The molecular orbitals of the AB_2 triatomic are obtained by mixing the central atom atomic orbitals with oxygen group orbitals of the appropriate symmetry. Thus, the a_1 σ-type group orbital is mixed with the a_1 sp_σ^2 atomic hybrid orbital to generate the $a_1\sigma_1$ bonding and σ_3 anti-bonding orbitals. In a similar fashion, the b_1 π-group orbital is mixed with the b_1 p_π atomic orbital to yield the $b_1\pi_0$ bonding and the π_2 anti-bonding orbitals. The a_2 π-type and b_2 σ-type group orbitals do not mix with the central atom atomic orbitals and are, therefore, essentially non-bonding orbitals with respect to the AB bond.

The energy of σ_3, the highest filled orbital of the 18-electron configuration, increases rapidly with bond angle as does the energy of the π_2 orbital, although less rapidly. Therefore, the $\sigma_3 \rightarrow \pi_2$ transition is expected to be accompanied by a large increase in the OPO bond angle as pointed out by Walsh [76] and Mulliken [77]. The three long wavelength electronic excitations of this configuration are illustrated in fig. 6. Of these

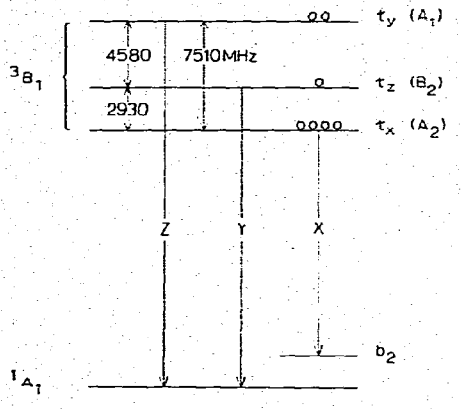

Fig. 7. Spin-orbital energy level diagram for the lowest triplet (B_1) of PO_2^- indicating the approximate relative steady state spin populations at 4.2 K and allowed electric dipole transitions.

transitions, only the $\pi_1 \rightarrow \pi_2$, $^1B_2 \rightarrow {}^1A_1$ and the $\sigma_3 \rightarrow \pi_2$, $^1B_1 \leftarrow {}^1A_1$ transitions are electric dipole allowed and of these two only the former is expected to have appreciable electric dipole intensity, due to the intrinsic overlap forbiddeness of a $\sigma \rightarrow \pi$ transition. Not illustrated in fig. 6, but of importance to a complete analysis of the phosphorescence spectrum, is the intense $\pi_0 \rightarrow \pi_2$, $^1A_1 \leftarrow {}^1A_1$ transition which is expected to lie to shorter wavelengths of 2000 Å.

The room temperature absorption spectrum of single crystals of phosphorus activated potassium chloride exhibits only a single broad absorption maximum at approximately 2900 Å corresponding to the $\sigma_3 \rightarrow \pi_2$, $^1B_1 \leftarrow {}^1A_1$ transition. This transition may be observed in greater detail in the low temperature phosphorescence excitation spectrum illustrated in fig. 1. Only a single vibrational progression was observed with an interval of 840 cm^{-1} which is most probably associated with the bending mode of the $^1B_1$ state. Other workers [58,59] have reported an additional vibrational interval of 363 cm^{-1} in the excitation spectrum which we were unable to observe, even though the resolving power of the excitation monochromator was well within the bandwidth of the observed vibrational structure. The electronic origin of the $^1B_1 \leftarrow {}^1A_1$ transition taken as the maximum of the first peak in the vibrational envelope is at 33 300 cm^{-1}.

The intense $\pi_1 \rightarrow \pi_2$, $^1B_2 \leftarrow {}^1A_1$ transition evidently lies to shorter wavelengths of 2000 Å in PO_2^-, as it also does in SO_2 and NO_2^-. The vibrationally allowed $\sigma_2 \rightarrow \pi_2$, $^1A_2 \leftarrow {}^1A_1$ transition is evidently too weak to be observed in absorption in dilute crystals as are the spin-forbidden transitions.

According to the above discussion, the lowest triplet state of an AB_2 18-electron molecule or ion would be of orbital symmetry B_1. The individual spin-orbital states illustrated in fig. 7 are, therefore, $A_1(\tau_y)$, $A_2(\tau_x)$ and $B_2(\tau_z)$. The three spin-orbital states of the triplet manifold gain transition dipole intensity to the ground state by direct or vibronic spin–orbit coupling mechanisms with one of the three lowest lying allowed singlet states. These are, in order of increasing energy, the $^1B_1$, $^1B_2$ and $^1A_1$ states and the principal direct spin–orbit (H_{so}) or vibronic spin–orbit (H_{vso}) coupling matrix elements between these singlet states and the individual spin-orbital states of $^3B_1$ are:

$$\langle {}^1B_2|H_{so}|B_2\rangle \rightarrow \langle p_y|\hat{L}_z|p_x\rangle_B, \tag{1a}$$

$$\langle {}^1A_1|H_{so}|A_1\rangle \rightarrow \langle p_z|\hat{L}_y|p_x\rangle_{A\,and\,B}, \tag{1b}$$

$$\langle {}^1B_1|H_{vso}|A_2\rangle \rightarrow \langle p_z|\hat{L}_x|p_y\rangle_B. \tag{1c}$$

The atomic matrix elements listed above were obtained by expanding the molecular spin–orbit coupling matrix elements in terms of the one-electron atomic spin–orbit coupling matrix elements and retaining only the one center terms. $\hat{L}_x$, $\hat{L}_y$ and $\hat{L}_z$ refer to the active components of the spin–orbit coupling operator, and the subscripts A and B designate the atomic centers of the matrix elements.

In general, we expect the magnitude of the vibronic spin–orbit coupling matrix element (1c) to be several orders of magnitude less than that of the direct spin–orbit coupling matrix elements [(1a) and (1b)]. Since the $^1A_1$ state of PO_2^-, by analogy to SO_2 and NO_2^-, is expected to be considerably higher in energy than the $^1B_2$ state, we expect matrix element (1a) to be of greater importance in radiative decay of $^3B_1$ than (1b). Thus, τ_z is predicted to be the most radiative spin-orbital state and emission from the $^3B_1$ state should be dominantly y-axis polarized. This conclusion is supported by Zeeman effect and optical polarization measurements on the emission of NO_2^-. It is of interest that the phosphorescence lifetimes of PO_2^- (2 ms), SO_2 (2.4 ms) and NO_2^- (3.1 ms) are very nearly identical, although the atomic spin–orbit coupling of phosphorus and sulfur are approximately 30 times

greater than that of nitrogen. This behavior supports the conclusion that the radiative decay of $^3B_1$ is dominated by matrix element (1a), which is localized on the oxygen atoms. Finally, we note that the fluorescence to phosphorescence quantum yield ratio ϕ_F/ϕ_P is zero for PO_2^- and approximately 50 for NO_2^-, indicating that the intersystem crossing rate depends upon spin–orbit coupling matrix elements on the central atom to some extent.

4.2. PMDR and lifetime measurements

Monitoring the most intense zero-phonon band at approximately 4090 Å (see fig. 1), two moderately strong ODMR signals were observed at 2930 MHz and 4580 MHz, both corresponding to an increase in phosphorescence intensity. A third, much weaker resonance signal could be observed at 7510 MHz either by simultaneously pumping (EEDOR) the 2930 MHz resonance or by monitoring the total phosphorescence intensity.

The PMDR spectra illustrated in fig. 1 are useful in confirming the details of the vibrational assignments and spin-orbital state origins of phosphorescence. The 4580 MHz PMDR which is not illustrated is similar in its appearance to the 2930 MHz PMDR. Both spectra correspond to an increase in intensity with microwave power, consistent with the relative population distributions illustrated in fig. 7, if it is assumed that, in agreement with theory, the most active spin state is τ_z.

The 7510 MHz spectrum selects the two relatively dipole inactive spin-orbital states τ_x and τ_y, and its interpretation presents an apparent dilemma. A change in sign of the signal occurs at the $\nu_3(b_2)$ vibronic origin which can best be rationalized by assuming that one of the two resonant spin-orbital states decays by a vibronic spin–orbit coupling mechanism, while the other decays via a direct spin–orbit coupling mechanism. By examination of matrix elements (1b) and (1c), we may conclude that τ_x decays principally by the vibronic mechanism, whereas τ_y decays predominantly by a direct spin–orbit coupling mechanism. The relative magnitudes of the positive and negative signal excursions in the 7510 MHz PMDR require the matrix elements (1c) and (1b) to be of comparable magnitude, whereas it is usually anticipated that the vibronic mechanism should be several orders of magnitude less effective in producing radiative decay to the ground electronic state.

The vibronic spin–orbit coupling mechanism appears to be also of considerable importance in the $^3B_1(\tau_x) \leftarrow {}^1A_1$ absorption of SO_2 vapor and $NaNO_2$ solid. In the SO_2 spectrum the $\nu_3(b_2)$ vibronic origin is observed with intensity comparable to that of the electronic origin. Van der Waals [78] has suggested that, in the case of SO_2, the vibronic spin–orbit coupling mechanism may be of increased importance because of the relatively low energy of the coupled $^1B_1$ state. Tinti [48] has observed the activity of $\nu_3(b_2)$ in the low temperature phosphorescence PMDR spectrum of SO_2 solid and identified the spin-orbital state origin as either τ_x or τ_y.

The lifetimes of the individual spin states were obtained by the method of microwave induced delayed phosphorescence by exciting the 2930 MHz and 4580 MHz resonances. The experimental decay curves are shown in fig. 4. The logarithms of the peak MIDP intensity are plotted versus delay time in fig. 3 and yield lifetimes of $\tau_y \approx \tau_x \approx 90$ ms and $\tau_z = 2$ ms. These results are in approximate agreement with those obtained by Avarmaa [58] from a graphical decomposition of the low temperature total phosphorescence decay, curve (a) in fig. 3. The above observations are consistent with the relative spin-orbital energy level and dipole activity scheme depicted in fig. 7.

4.3. Vibrational analysis

Since no salts of the PO_2^- anion are known, the P–O bond length and the OPO angle in the electronic ground state are not available from crystal structure data, and we have attempted to obtain structural information from the observed normal mode frequencies assuming a valence force field model. Additionally, we have calculated the structure of the ion in the lowest triplet electronic excited state by a quantitative application of the Franck–Condon principle to the observed vibronic intensity distributions in the electronic emission spectrum.

A complete calculation of the ground and excited state geometries from the vibrational analysis of the infrared and electronic spectra was not possible, due to the incomplete set of natural and isotopic normal mode frequencies obtained. We have available from our work and that of others, the vibrational frequencies of

Table 1

	PO_2^-	SO_2	NO_2^-	O_3
Central atom electronegativity [79]	2.19	2.58	3.04	3.44
$^1B_2$ (cm^{-1})	–	41413 [80]	≈48780 [81]	–
ν_1	–	963 [80]	–	–
ν_2	–	377 [80]	–	
ν_3	–			
$^1A_2$	–	~35700 [82]	≈33300 [81]	–
$^1B_1$	33051 [59]	29622 [80]	25977 [83]	–
ν_1	840	764 [80]	1018 [40]	–
ν_2	363 [59]	317.5 [80]	632 [40]	–
ν_3	–	813 [80]	–	–
$2\Delta\alpha$ (°)	–	–	9 [84]	–
$^3B_1$ (cm^{-1})	24924	26385 [47]	18959 [40]	10000 [80]
ν_1	–	918 [47]	1124 [40]	–
ν_2	400 [59]	382 [47]	644 [40]	566.7 [80]
ν_3	–	–	1170 [40]	–
$2\Delta\alpha$ (°)	7.3	7.8 [47]	14 [40]	–
ΔAB (Å)	0.065	0.042 [47]	–	–
$^1A_1$ (cm^{-1})				
ν_1	1097	1147 [47]	1325 [40]	1110 [84]
ν_2	501	521 [47]	831 [04]	705 [84]
ν_3	1207	1330 [47]	1243 [40]	1042 [84]
2α (°) [84]	(110) [a]	119.5 (120)	116	117
d_{AB} (Å) [84]	1.65	1.432	1.23	1.276

[a] Values in parentheses are computed using the valence force potential.

the PO_2^- ion in the ground state ($^1A_1$). Additionally, we have available the frequencies of the two ground state totally symmetric modes of the isotopically substituted species $[P^{16}O^{18}O]^-$. The totally symmetric bending frequency of the $^3B_1$ state and of the first $^1B_1$ state have also been reported [59].

Using only the frequencies of the normal modes of the naturally abundant isotope it is possible to calculate a theoretical value of the OPO bond angle as well as the potential energy constants in the valence force potential: $2V = k_1 S_1^2 + (k_\theta/R_0^2)S_2^2$. The results are $2\theta = 109.6°$, $k_1 = 8.124 \times 10^5$ g s^{-2} and $k_\theta/l^2 = 0.807 \times 10^5$ g s^{-2}. The valence force model has been quite successful in predicting the bond angle in other isoelectronic AB_2 type molecules as demonstrated in table 1, and we feel reasonably confident in its use to compute a value of the bond angle for PO_2^-. For the purposes of calculating the excited state geometry of the PO_2^- ion from the vibrational analysis of the phosphorescence spectrum, we have adopted the procedure employed by Coon et al. [85] in a similar calculation for SO_2. We define symmetry coordinates for the totally symmetric deformations of PO_2^- as:

$$S_1 = \Delta R_0, \qquad S_2 = 2R_0\Delta\theta, \tag{2}$$

where R_0 is the equilibrium P–O bond length and $\Delta\theta$ is the change in the OPO bond angle. The symmetry coordinates are related to the ground state normal coordinates of the symmetric stretching and bending modes Q_1 and Q_2, respectively, by the coordinate transformation:

$$S = LQ, \tag{3}$$

where S and Q are two component column vectors and L is a 2×2 matrix whose elements are obtained from the observed eigenfrequencies, the equilibrium OPO bond angle and the valence force potential constants, upon solving a two dimensional secular determinant. The relative contribution of each symmetry coordinate to the normal modes Q_1 and Q_2 are obtained from the relation:

$$Q = L^{-1}S. \quad (4)$$

Thus:

$$Q_1 = (0.4271\,S_1 - 0.0278\,S_2) \times 10^{-11},$$

$$Q_2 = (0.3461\,S_1 + 0.5291\,S_2) \times 10^{-11}. \quad (5)$$

The normal mode Q_2 is seen to consist of approximately equal amounts of the S_1 and S_2 symmetry coordinates, while the normal mode Q_1 is accurately described by the S_1 stretching symmetry coordinate alone.

Using the results from the normal coordinate analysis we may determine the approximate geometry of the first triplet electronic excited state of PO_2^-. In order to obtain accurate relative intensity measurements of the zero-phonon lines, it was necessary to correct the spectrum shown in fig. 1 for wavelength variations in the response of the detection system. This was accomplished by using a standard 200 W quartz-halogen lamp of known spectral irradiance [86]. We then obtain from the observed intensity distributions in the vibrational progressions of the crystal phosphorescence spectrum the normal coordinate displacements d_1 and d_2 between the ground and first excited triplet state by a quantitative application of the Franck–Condon principle. In this calculation, we assume that the normal coordinates of the ground and excited electronic states remain parallel. At 4.2 K emission occurs from the lowest vibrational level of the excited state and we may write:

$$\frac{I(0, \nu_n^i)\nu_{00}^4}{I(0,0)\nu_{0n}^4} = \frac{|\langle\phi_0^i|\phi_n^i\rangle|^2}{|\langle\phi_0^i|\phi_0^i\rangle|^2}, \quad (6)$$

where i represents the normal mode under consideration, 0 designates the vibrational level of the ground state, and ϕ_n is the vibrational wavefunction of the nth level. Equations for the individual vibrational overlap integrals can be generated using the general formula available in the literature. The overlap integrals are dependent upon two parameters,

$$\beta_i = \nu_i''/\nu_i', \quad \gamma_i = (4\pi^2\nu_i' c/\hbar)^{1/2} d_i, \quad (7)$$

where ν_i'' and ν_i' are the ground and excited state normal mode frequencies of the ith mode, respectively, and d_i is the displacement of the excited state potential minimum relative to the ground state potential minimum. In the case of the stretching mode, only three lines of adequate intensity were available and, although this is sufficient for an algebraic determination of the parameters, no check on their accuracy was possible. The bending mode, however, furnished five usable lines and these were fit to 4% precision by variation of β and γ. The normal coordinate displacements obtained by this procedure are:

$$d_1 = 0.258 \times 10^{-20}\ \mathrm{g}^{1/2}\ \mathrm{cm},$$

$$d_2 = 0.576 \times 10^{-20}\ \mathrm{g}^{1/2}\ \mathrm{cm}.$$

The change in the PO bond length and OPO bond angle upon excitation to the $^3B_1$ state was calculated from the relation:

$$S' = LQ' = L(Q + D), \quad (8)$$

by setting $Q = 0$. The results of this procedure are given in table 1 where they are compared with the results of a similar calculation for the isoelectronic ion NO_2^- and molecule SO_2. It should be noted that the sign of the displacement is not determined in these experiments. It is assumed that the change in bond angle associated with d_2 corresponds to an increase, as suggested by the arguments put forward by Walsh [76] and Mulliken [77] and summarized in the above discussion.

4.4. Isotope effect

The isotope shift of the molecular frequencies provides considerable information about the chemical and structural nature of the site. The observation (fig. 2) of an isotope splitting of the phosphorescence lines in crystals enriched with ^{18}O confirms the participation of oxygen in the formation of the impurity center. The exact mechanism of formation of the PO_2^- center is uncertain. It seems probable that reaction occurs between crystal O_2^- centers and atomic phosphorus in situ at elevated temperatures only slightly below the melting point of potassium chloride. However, when crystals containing only $(^{18}O)_2^-$ centers were heated in phosphorus vapors in evacuated silica tubes, the emission spectrum obtained showed considerable contamination by ^{16}O. The only apparent source of the naturally abundant isotope is the vitreous silica tube used to activate the samples. Since, in the preparation of the $(^{18}O)_2^-$ doped potassium chloride crystals no exchange with the silica was observed, the pro-

Table 2
Vibronic analysis

Assignment	$[P^{16}O_2]^-$	$[P^{18}O^{16}O]^-$
$1_0 2_0 2_0$	24 923 cm^{-1}	(24 923) [a]
2_1	24 422	24 435
2_2	23 921	23 946
1_1	23 826	23 860
3_1	23 716	–
2_3	23 418	23 452
$1_1 2_1$	23 331	23 371
2_4	22 919	22 964
$1_1 2_1$	22 834	22 885
1_2	22 745	22 803

[a] Not observed as a separate line.

cess must be activated by the presence of phosphorous at elevated temperatures. Therefore, we conclude that during the phosphorus activation process, the phosphorus vapors attack the silica, liberating active oxygen which is rapidly exchanged with the O_2^- crystal centers. Examination of the silica tubes used in the activation procedure revealed considerable etching, apparently as a result of this process.

If during activation the ratio of isotopic concentrations is $R = [^{18}O]/[^{16}O]$, then the resulting ratio of the concentrations of the isotopically enriched ions $(P^{16}O_2)^- : (P^{16}O^{18}O)^- : (P^{18}O_2)^-$ will be $1 : 2R : R^2$. Only two isotopic species are observed in the emission spectra with an intensity ratio of approximately 7 : 1, suggesting that $R = 1/14$. The intensity of the symmetrically substituted species $(P^{18}O_2)^-$ would have been about 1/200 that of the naturally abundant isotope and below the detection limits under the conditions of the experiment.

The ground state symmetric mode frequencies for the various isotopic ions were obtained from the vibronic analysis of the phosphorescence spectrum. The frequency of ν_3, the non-totally symmetric stretch, was obtained accurately from the infrared spectrum of phosphorus activated crystals which exhibited only a single absorption band at 1207 cm^{-1}. The observed isotope frequency shifts are given in table 2. For comparison with theory, the frequency ratio may be compared with that calculated by means of the following equation.

$$\frac{\nu_1^{\mathrm{i}}\nu_2^{\mathrm{i}}}{\nu_1\nu_2} = \left[\frac{(2M_{\mathrm{O}}^{\mathrm{i}} + M_{\mathrm{P}})(M_{\mathrm{O}})^2}{(2M_{\mathrm{O}} + M_{\mathrm{P}})(M_{\mathrm{O}}^{\mathrm{i}})^2}\right]^{1/2}. \qquad (9)$$

The superscipt (i) stands for the isotopic molecule; M_{O} and M_{P} are the masses of oxygen and phosphorus atoms, respectively; and ΔM_{O} is the mass difference between ^{16}O and ^{18}O. The equation given is that for the isotope product ratio of the symmetrically substituted C_{2v} ion. For the a_1 modes, the value of $\nu_1^{\mathrm{i}}\nu_2^{\mathrm{i}}/\nu_1\nu_2$ is calculated to be 0.9167, in poor agreement with the experimental value of 0.9530. The lack of agreement suggests that the experimentally observed isotope splitting is, in fact, that of the asymmetrically substituted ion. The corresponding relationship for the asymmetrically substituted ion is considerably more complicated than that for the C_{2v} ion. However, since $[\Delta M_{\mathrm{O}}/M_{\mathrm{O}}]^2 \ll 1$, we may obtain to good approximation the corresponding quantity for the asymmetrically substituted ion by assuming the isotope shifts to be half those of the symmetrically substituted species. The calculated value of the isotope product ratio for the a_1 modes of the asymmetrically substituted ion of 0.9554 is then in excellent agreement with the experimental value. We conclude that the symmetrically substituted species, as suggested previously, was present in concentration too low to be observed.

4.5. Comparison with other molecules

There are numerous spectroscopic studies of symmetrical AB_2 triatomic molecules and ions which are isoelectronic with the 18-electron PO_2^- structure, and it is of some interest to compare and contrast the spectroscopic results obtained for PO_2^- with those obtained for various other 18-electron triatomic molecules. Such a comparison is facilitated by use of the well known Walsh diagram for these molecules and ions, which conveniently summarizes the qualitative aspects of a crude molecular orbital treatment.

The known transition energies and geometrical data for the 18-electron symmetrical triatomic molecules and ions of the isoelectronic, isovalent series:

$$[PO_2^-, SO_2, NO_2^-, O_3] \qquad (10)$$

are collected in table 1. Note that the B-type atoms are in each instance oxygen and that the various molecules and ions of this series are listed in order of increasing electronegativity of the A-type atom or, alternatively, in order of increasing valence orbital ionization energy.

In order to rationalize the behavior of the long wavelength transitions of the series, we begin by noting

that both π_1 and σ_2 are almost wholly localized on the oxygen atoms and, therefore, independent energetically of the character of the central atom. Conversely, the energy of the σ_3 and π_3 molecular orbitals depends critically upon the details of the group-orbital–atomic orbital interaction.

This interaction is large for the σ orbital mixing, due in part to the large orbital overlap. Therefore, the energy of the σ_3 orbital is determined principally by the off-diagonal resonance-type matrix elements of the secular determinant, which are greatest when the difference in electronegativity between the central atom and oxygen is least. Thus, σ_3 lies highest in energy for O_3 and lowest for PO_2^-.

The energy of the π_2 molecular orbital is determined principally by the diagonal or Coulomb-type matrix elements of the secular determinant and, therefore, varies inversely as the electronegativity of the central atom, lying highest in energy for PO_2^- and lowest for O_3.

We anticipate, on the basis of these arguments, that the $\pi_1 \rightarrow \pi_2$, $^1B_2 \leftarrow {}^1A_1$ transition is found to longer wavelengths in the order of the series (13). The same conclusion may be reached for the $\sigma_3 \rightarrow \pi_2$, $^1B_1 \leftarrow {}^1A_1$ transition, with the additional comment that this transition should shift more rapidly along the series than the former. These conclusions are in reasonable agreement with the available experimental measurement summarized in table 1.

References

[1] K.K. Rebane and L.A. Rebane, J. Pure Appl. Chem. 37 (1974) 161.
[2] A. Freiberg and L.A. Rebane, Phys. Stat. Sol. 81 (1977) 359.
[3] W. Kanzig, J. Phys. Chem. Solids 23 (1962) 479.
[4] M. Ikezawa and J. Rolfe, J. Chem. Phys. 58 (1973) 2024.
[5] L.A. Rebane and A.B. Treshchalov, J. Luminescence 12/13 (1976) 425.
[6] J.M. de Siebenthal and H. Bill, Phys. Stat. Sol. 79 (1977) 259.
[7] H. Bill and W. von der Osten, Phys. Stat. Sol. 75 (1976) 613.
[8] J. Rolfe, F.R. Lipsett and W.J. King, Phys. Rev. 123 (1961) 447.
[9] H.R. Zeller, R.T. Shuey and W. Kanzig, J. Phys. Suppl. C4 (1967) 81.
[10] A.M. Freiberg and L.A. Rebane, Soviet Phys. Solid State 16 (1975) 1704.
[11] J. Rolfe, J. Chem. Phys. 40 (1964) 1664.
[12] L.A. Rebane, O.I. Sil'd and T.Yu. Khal'dre, Akad. Nauk SSSR, Bull. Phys. Ser. 35 (1971) 1276.
[13] K.K. Rebane, A.I. Laisaar, L.A. Rebane and O.I. Sil'd, Akad. Nauk SSSR, Bull. Phys. Ser. 31 (1967) 2053.
[14] L.A. Rebane and P.M. Saari, Soviet Phys. Solid State 12 (1971) 1547.
[15] W. Kanzig and M.H. Cohen, Phys. Rev. Letters 3 (1959) 509.
[16] K.K. Rebane, L.A. Rebane and O. Sild, Proceedings of the International Conference on Luminescence (1966) p. 860.
[17] L.A. Rebane, A.B. Treshchalov and T.Yu. Khal'dre, Soviet. Phys. Solid State 16 (1975) 1460.
[18] V.R. Kumeskii and I.Ya. Kushnirenko, Akad. Nauk SSSR Bull. Phys. Ser. 34 (1970) 474.
[19] M.U. Belyi, V.R. Kumeskii and I.Ya. Kushnirenko, Akad. Nauk SSSR, Bull. Phys. Ser. 35 (1971) 1285.
[20] W.D. Seward and V. Narayanamurti, Phys. Rev. 148 (1966) 463.
[21] J.H. Schulman and R.D. Kirk, Solid State Commun. 2 (1964) 105.
[22] M.J. Marrone, F.W. Patten and M.N. Kabler, Phys. Rev. Letters 31 (1973) 467.
[23] A. Wasiela, G. Ascarelli and Y. Merle d'Aubigne, Phys. Rev. Letters 31 (1973) 993.
[24] M.N. Kabler, M.J. Marrone and W.B. Fowler, Luminescence of crystals, molecules and solutions, ed. F. Williams (Plenum Press, New York, 1973).
[25] J.U. Fischbach, D. Frohlich and M.N. Kabler, J. Luminescence 6 (1973) 29.
[26] M.J. Marrone and M.N. Kabler, Phys. Rev. Letters 27 (1971) 1283.
[27] W.B. Fowler, M.J. Marrone and M.N. Kabler, Phys. Rev. B (1973) 5909.
[28] T. Yoshinari and M. Hirai, J. Phys. Soc. Japan 39 (1975) 720.
[29] M.N. Kabler and D.A. Patterson, Phys. Rev. Letters 19 (1967) 652.
[30] R.B. Murray and F.J. Keller, Phys. Rev. 137 (1965) A942.
[31] T. Yoshinari and M. Hirai, J. Phys. Soc. Japan 39 (1976) 1498.
[32] M.N. Kabler, Phys. Rev. 136 (1964) A1296.
[33] J. Ramamurti and K. Teegarden, Phys. Rev. 145 (1966) 698.
[34] H. Takezoe and R. Onaka, J. Luminescence 12/13 (1976) 419.
[35] A.R. Evans and D.B. Fitchen, Phys. Rev. B 2 (1970) 1074.
[36] R.M. Hochstrasser and A.H. Zewail, J. Chem. Phys. 54 (1971) 2979.
[37] V. Narayanamurti, W.D. Seward and R.O. Pohl, Phys. Rev. 148 (1966) 481.
[38] H.J. Maria, A.T. Armstrong and S.P. McGlynn, J. Chem. Phys. 48 (1968) 4694.
[39] W.C. Allen and R.N. Dixon, Trans. Faraday Soc. 65 (1968) 1168.
[40] R.M. Hochstrasser and A.P. Marchetti, J. Chem. Phys. 50 (1969) 1727.

[41] L.A. Rebane, G.S. Zavt and K.E. Haller, Phys. Stat. Sol. 81 (1977) 57.
[42] R. Avarmaa and L. Rebane, Phys. Stat. Sol. 35 (1969) 107.
[43] R. Bonn, R. Metselaar and J. van der Elsken, J. Chem. Phys. 46 (1967) 1988.
[44] T. Timusk and W. Staude, Phys. Rev. Letters 13 (1964) 373.
[45] J.U. von Schutz and W. Dietrich, Chem. Phys. Letters 51 (1977) 418.
[46] J. Schneider, B. Dischler and A. Rauber, Phys. Stat. Sol. 13 (1966) 141.
[47] R.M. Hochstrasser and A.P. Marchetti, J. Mol. Spectry. 35 (1970) 335.
[48] D.S. Tinti, Chem. Phys. Letters 12 (1971) 169.
[49] J. Suwalski and H. Seidel, Phys. Stat. Sol. 13 (1966) 159.
[50] J.R. Brailsford and J.R. Morton, J. Mag. Resonance 1 (1969) 575.
[51] B. Meyer, L.F. Phillips and J.J. Smith, Proc. NAS 61 (1968) 7.
[52] H. Zeldes and R. Livingston, J. Chem. Phys. 35 (1961) 563.
[53] N.M. Atherton, R.N. Dixon and G.H. Kirby, Trans. Faraday Soc. 60 (1964) 1688.
[54] J.W. Rabalais, J.R. McDonald and S.P. McGlynn, J. Chem. Phys. 51 (1969) 5095.
[55] I.Ya. Kushnirenko, Akad. Nauk SSSR, Bull. Phys. Ser. 32 (1968) 1305.
[56] G.W. Chantry and D.H. Whiffen, Mol. Phys. 5 (1962) 189.
[57] E. Wasserman, L. Barash and W.A. Yager, J. Am. Chem. Soc. 87 (1965) 2075.
[58] R.A. Avarmaa, Izv. Akad. Nauk SSSR, Bull. Phys. Ser. 36 (1972) 962.
[59] R.A. Avarmaa, Opt. Spectry. 32 (1972) 514.
[60] S.J. Hunter, K.W. Hipps and A.H. Francis, Chem. Phys. Letters 51 (1977) 287.
[61] B.T. Plachenov, V.P. Avdonin, V. Kapishovskii and G.A. Mikhal'chenko, Izv. Akad. Nauk SSSR, Bull. Phys. Ser. 31 (1967) 2067.
[62] B.T. Plachenov, V.P. Avdonin, G.A. Mikhal'chenko and V.M. Smagin, Izv. Akad. Nauk SSSR, Bull. Phys. Ser. 30 (1966) 1474.
[63] J.M. de Siebenthal and H. Bill, Chem. Phys. Letters 45 (1977) 334.
[64] J. Schmidt, W.S. Veeman and J.H. van der Waals, Chem. Phys. Letters 4 (1969) 341.
[65] D.A. Antheunis, J. Schmidt and J.H. van der Waals, Chem. Phys. Letters 6 (1970) 255.
[66] T.S. Kuan, D.S. Tinti and M.A. El-Sayed, Chem. Phys. Letters 4 (1970) 507.
[67] D.S. Tinti, M.A. El-Sayed, A.H. Maki and C.B. Harris, Chem. Phys. Letters 3 (1969) 343.
[68] J. Schmidt and J.H. van der Waals, Chem. Phys. Letters 2 (1968) 640.
[69] M. Sharnoff, J. Chem. Phys. 46 (1967) 3263.
[70] J. Schmidt, I.A.M. Hesselmann, M.S. de Groot and J.H. van der Waals, Chem. Phys. Lett. 1 (1967) 434.
[71] A.L. Kwiram, Chem. Phys. Letters 1 (1967) 272.
[72] R. Hilsch and R.W. Pohl, Z. Physik 57 (1929) 145.
[73] R. Hilsch and R.W. Pohl, Z. Physik 59 (1930) 812.
[74] R. Hilsch and R.W. Pohl, Z. Physik 48 (1928) 384.
[75] B. Gudden and R. Pohl, Z. Physik 44 (1927) 860.
[76] A.D. Walsh, J. Chem. Soc. 467 (1953) 2266.
[77] R.S. Mulliken, Rev. Mod. Phys. 14 (1942) 204.
[78] J.H. van der Waals, Discussions Faraday Soc. 35 (1963) 227.
[79] W.J. Moore, Physical chemistry (Prentice-Hall, New Jersey, 1972).
[80] G. Herzberg, Electronic spectra and electronic structure of polyatomic molecules (Van Nostrand, Princeton, 1966).
[81] W.H. Eberhardt and W.G. Trawick, J. Chem. Phys. 22 (1954) 1462.
[82] S.J. Strickler and D.B. Howell, J. Chem. Phys. 49 (1968) 1947.
[83] J.W. Sidman, J. Am. Chem. Soc. 79 (1957) 2669.
[84] J.W. Sidman, J. Am. Chem. Soc. 79 (1957) 2675.
[85] J.B. Coon, R.E. de Wames and C.M. Loyd, J. Mol. Spectry. 8 (1962) 285.
[86] R. Stair, W.E. Schneider and J.K. Jackson, Appl. Opt. 2 (1963) 1151.